Journal of Information Systems Engineering and Management
2024, 9(4)
e-ISSN: 2468-4376
https://www.jisem-journal.com/

Research Article

FOPID-PI Controlled 31-Level Multilevel Inverter for Stability Improvement of Islanded Single-Phase Community Microgrid

Sridevi A*[1], H. R. Ramesh[2]
*[1]*Research Scholar, Department of Electrical Engineering, University Visvesvaraya College of Engineering, K R Circle, Bangalore, Karnataka 560001, India.*
[2]*Professor & Chairman, UVCE, K R Circle, Bangalore, Karnataka 560001, India.* **Email: sridevia712@gmail.com*

ARTICLE INFO

Article Received: 03/10/2024
Article Revised: 22/10/2024
Article Accepted: 12/11/2024

ABSTRACT

These days, the majority of distribution generation comes from renewable energy sources because of their benefits, which include being pollution-free and low carbon. Concurrently, the issue emerged because of the sources' non-linearity over time. Therefore, the maximum power point tracking (MPPT) controller based on artificial neural networks (ANN) is employed. The ANN-based MPPT controller in this proposed work receives the voltage and current from the solar panel and uses it to control the best switching pulses to send to the DC-DC converter, which in turn feeds the MLI and improves stability. This study builds a single-phase, 31-level asymmetrical MLI with three uneven DC voltage sources and fewer sources. In order to regulate the performance of the MLI, this work suggests a cascaded fractional order proportional integral derivative (FOPID) and proportional integral (PI) controller. The performance of the proposed methodology is verified using an islanded single phase microgrid with an AC load and a MATLAB/SIMULINK tool. According to the results, the suggested inverter outperformed the present 31 level inverter topologies in terms of Total Harmonic Distortion (THD), achieving lower values of 2.95% and 0.75% for voltage and current, respectively. With decreased THD, the suggested 31-level inverter achieved a high efficiency of 96.62%.

Keywords: ANN based MPPT, DC-DC converter, duty cycle, total harmonic distortion (THD), Multi-level inverter (MLI), switching pulses, fractional order proportional integral derivative (FOPID) proportional integral (PI) and stability.

1. Introduction

A number of factors, such as the growing demand for energy, environmental concerns, the need to lower the cost of producing electricity, and the requirement to improve the reliability of electric systems, have contributed to the recent rapid increase in distributed energy resources (DERs) in electric networks [1-2]. In the near future, most homes should have distributed energy resources (DERs), mostly in the form of single-phase, grid-connected solar, wind, fuel cell, or battery systems [3]. Renewable energy sources (RESs), such solar and wind turbines, as well as battery energy storage devices, are commonly used in low voltage grids, which produce energy closer to the user [4]. Energy sources and loads that function similarly have led to the formation of single-phase and three-phase low voltage microgrids. These microgrids maximize energy efficiency and improve the local electrical network's dependability [5, 6].

Because solar energy requires minimal maintenance, is environmentally beneficial, and is readily available, it is the most popular renewable energy source [7]. However, compared to other power networks, the output voltage of solar photovoltaic (PV) arrays is far lower. To increase the system's output voltage, a maximum power point tracking (MPPT) DC-DC converter has been incorporated [8]. RES based MPPT is integrated with a power converter to track high power from sources. Adding an MPPT controller will result in about 30% more power being produced [9]. This MPPT selects the optimal duty cycle to control the DC to DC converter

Research Article

[10]. For improved performance, a few authors combined MPPT with other neural networks and machine learning techniques. To achieve high power from PV, the author in [11] employed the machine learning approach with MPPT. Neuro fuzzy and terminal sliding mode control techniques are developed in [12] for two stage MPPT. Power from solar PV and wind integrated power systems was obtained using K-nearest neighbor based MPPT [13]. Recent studies have shown the efficacy of artificial intelligence (AI)-based methods have the potential to power tracking applications [14].

To convert DC to AC power dependent on loads, inverters are required; multi-level inverters (MLI) have become increasingly popular in recent years [15]. MLI working in the DC voltage source's input produces the multilayer output, which can be used for high, medium, or low level switching frequency PWM systems [16]. Three main forms of multi-level inverters are found in basic MLI architecture: diode clamped, capacitor-clamped, and cascaded H-bridge topology [17, 18].Power quality is negatively impacted by the creation of such high voltage levels, irrespective of the design [19]. Furthermore, a major challenge for Stability is dependability issues caused by a high number of switches [20]. Stabilityhas been improved by producing the pulses utilizing the best control procedures. This research reduced the stability issue, such as excessive harmonics in MLI, by introducing a revolutionary inverter with fewer switches and an optimal controller. Author in [36] suggested a PV powered EV charging station using a SEPIC integrated isolated flyback converter with RBFNN based MPPT and a 31-level inverter to enhance efficiency and reliability. Author in [37] have suggested an SM-CNN based 31-level multilevel inverter and a boost converter to improve the model performance.Author in [38] a sliding mode controller based multilevel inverter with a gravitational search algorithm for MPPT and a cascaded interleaved boost converter to optimize grid connected PV power systems with enhanced efficiency.

The main objective of this paper is as follows;

- To develop a 31-level multilevel inverters with a minimum number a switches and voltage sources to enhance the stability.
- To implement and ANN based MPPT controller to extract the maximum power from solar PV system by generating optimal switching signals.
- To enhance inverter stability and performance a hybrid cascaded controller is proposed for optimizing switching pulses.

The remaining sections are arranged below; section2 discussed recent literature on the MLI inverter and controllers. The proposed methodology with the inverter design is given in section3. Results are provided in section4, and the conclusion is given in section5.

2. Related Works

Recent literature for MLI modeling and controllers is listed below, In order to regulate the DC-link of the system, Nahin et al. [21] suggested utilizing ANN based MPPT for 3 level neutral point clamped MLI in induction motor drives. Furthermore, the inverter's THD was improved by injecting 60 degree PWM approach with 13th harmonics. The inverter will receive pulses from this PWM that are balanced and symmetrical. This technique increased the induction motor's stator current and voltage while lowering torque ripple.

Kumar et al. [22] introduced ANFIS-based MPPT to track high power from solar-fed PV panels. A single phase, 31-level inverter was created in this study. The switching pulses for this inverter were generated using ANN and a proportional integral controller. To achieve improved results at various operating points, the ANN algorithm was used to update the PI values.

Grey wolf optimization based recurrent neural network (GWO-RNN) was suggested by Prathaban et al. [23] for solar MPPT. The MPPT gadget with GWO-RNN based improved tracking capabilities and fast speeds. RNN networks and feed forward neural networks are not the same. RNNs will use their internal memory to process and carry out input sequences. Pulses were generated for the inverter using basic PWM.

Journal of Information Systems Engineering and Management
2024, 9(4)
e-ISSN: 2468-4376
https://www.jisem-journal.com/

Research Article

Fuzzy logic controller-based MPPT in a 31-level inverter with four DC sources is suggested by Kurian et al. [24]. A full bridge converter was utilized in this work to convert the DC output power to AC. The voltage range at which full-bridge inverters can be operated is restricted by their positioning. A brand-new 31-level MLI architecture for solar PV was provided by this study. To determine the class labels and induction technique for the fuzzy set, trial and error was employed.

An asymmetric 31-level MLI with twelve switches was suggested by Akther et al. [25] to reduce the size and THD. Every power switch in this suggested inverter operates in a unidirectional manner. To reach level 31, four DC sources with a ratio of 2:4:8:16 were utilized. Diodes are not utilized in order to prevent open circuit and short circuit failures. This suggested MLI was among the best for real-world, demanding inverters.
A novel 31 level micro inverter with a novel control strategy was recommended by Shah et al. [26] to reduce the THD. This technique extracts high power from solar energy using an MPPT based on perturb and observe (P&O). The power switching device's single half-bridge circuit was linked to the DC supply produced by the push-pull converter. One source can be divided into many DC sources using a push-pull converter. It makes use of a high-frequency transformer with four secondary windings and a center tap primary winding. It is decided which secondary winding turns will produce binary supply voltages of 12, 24, 48, and 96 V.

Modified packed u cell topology has been suggested by Krishnamoorthy et al. [27] to produce 31 level MLI. This topology is made up of voltages and switches connected in series and parallel. This suggested inverter has five voltage sources and ten power switches. This study offers a 31-level topology converter that was switched by a variable switching frequency-based model predictive controller to produce an optimal output with less harmonics. The gate driver circuit's size complexity and power consumption were optimized. Table 1 compares previous research based on MPPT topology in MLI and 31 level inverters.

Table 1: Comparative Analysis

Author	Level	Switches	THD	MPPT Methods	Limitations
Nahin et al. [21]	3	12	3.60, 4.70	ANN	Power quality was less.
Kumar et al. [22]	31	12	3.81, 3.86	ANFIS	Efficiency was not measured.
Prathaban et al. [23]	7	6	4.2	GWO-RNN	The size was increased due to the converter.
Kurian et al. [24]	31	14	0.962	Fuzzy logic controller	Not suitable for industrial applications.
Akther et al. [25]	31	12	6.72	-	Not applicable for high power appliances.
Shah et al. [26]	31	12	3.16, 0.82	P&O	Harmonics of voltage is high when compared to current.
Krishnamoorthy et al. [27]	31	10	3.27	-	Efficiency was less.

3. Proposed Methodology

Due to its distinct features over networked systems, such as the non-dispatchable nature of renewable resources and the inverter's dynamic control response the microgrid poses power quality difficulties. Microgrid stability is contingent upon both control topology and system structure. The circuit breaker disconnects the MG to allow for islanded operation when a grid fault arises. Subsequently, sources and battery units individually provide the loads at nominal voltage and frequency. As a consequence, this technique tracked high-power solar PV utilizing artificial neural network-based MPPT. Batteries have been utilized for high load demand and are used to store excess PV power.

Usually, a master-slave control method is used in the microgrid to synchronize the PV and battery units. In this manner, the PV is regarded as the slave unit and the battery as the master unit. In this work, a 31-level asymmetric multi-level MLI with fewer switches and DC sources is suggested. This suggested MLI's switching pulses are managed by a unique cascaded controller. The suggested cascaded controller structure, known as a

Journal of Information Systems Engineering and Management
2024, 9(4)
e-ISSN: 2468-4376
https://www.jisem-journal.com/

Research Article

C-FOPID-PI controller, is based on a proportional integral (PI) in the second stage and a fractional order proportional integral derivative (FOPID) in the first. The suggested controller uses the measured and reference voltages to determine which switching signals to send to the inverter. An islanded mode single phase microgrid system uses this suggested model.

3.1 System Description

The proposed architecture for a single-phase microgrid is shown in Figure 1. The slave PV unit and master battery comprise the proposed architecture. The common AC bus connects all the loads and distribution energy sources. The circuit impedance is disregarded by the simplified single-bus model due to the community microgrid's small footprint and short circuit length. Thus, there is no need for reference frame change. The proposed single phase MLI and filter with the proposed controller comprise the master unit. The master unit's inverter regulates the frequency and voltage of the common bus. An ANN-based MPPT, a proposed MLI, anLCLfilter, and an inverter controlled by a suggested controller approach comprise the slave unit. The proposed microgrid under evaluation is depicted in Figure 1. It consists of a slave solar unit and a master battery energy storage system (BESS). The signal is generated by the BESS and then monitored and filtered using a unique controller in the RES unit capacitor filter.

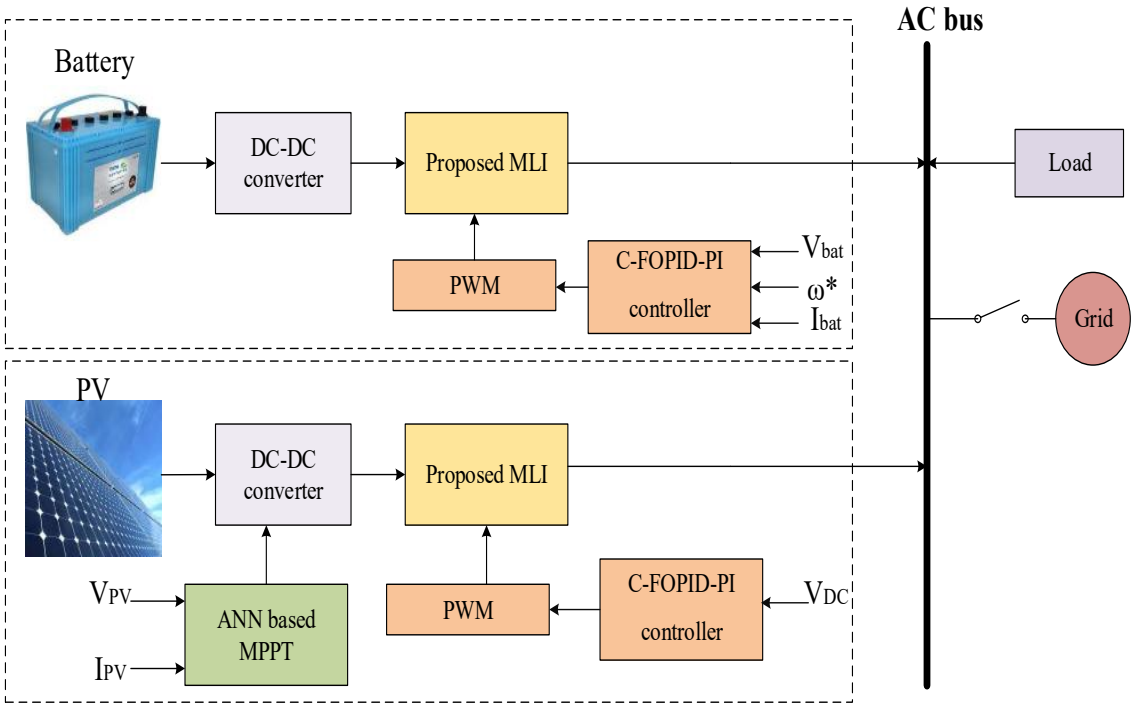

Figure 1: Structure of the proposed Microgrid under study

The primary goal of the slave unit is to control the output power, which will provide the necessary power to satisfy load demands. Any excess power produced by the photovoltaic system that is not used by the loads can be absorbed by the batteries. This leads to the following mathematical expression:

$$P_{Bat} = P_{load} - P_{PV} \qquad (1)$$

Where, P_{Bat} indicates available power in the battery, P_{load} denotes load demand, and P_{PV} specifies the power generated from PV. The power produced from solar PV is calculated using the following equation;

Journal of Information Systems Engineering and Management
2024, 9(4)
e-ISSN: 2468-4376
https://www.jisem-journal.com/

Research Article

$$P_{PV} = V_{PV}\left(I_{Ph} - I_0\left[e^{\frac{\left(V + I.R_S\right)}{V_t \lambda}} - 1 \right] - \frac{\left(V + I.R_S\right)}{R_P} \right) \qquad (2)$$

Where, I denotes the current from a single solar cell, V_{PV} represent output voltage, I_o indicates saturation current, T represent temperature, R_{series} indicates resistance in series, q signifies charge in electron, V_t denotes terminal voltage, k denotes Boltzmann constant, R_{shunt} represent parallel resistance, λ specifies identity factor, I_{Ph} means current generated using solar irradiance, V indicates open circuit voltage and a indicates diode factor [28]. Temperature and solar radiation are two environmental factors that affect the electricity generated by photovoltaic cells. Consequently, the PV injects all available power using the MPPT algorithm. Many contemporary control systems have been created to use MPPT to monitor high power in photovoltaic systems. In this work, high power PV is obtained by the application of ANN-based MPPT.

3.2 ANN based MPPT

Artificial neural networks (ANNs) are a class of statistical learning models that are used to estimate or approximate functions that have multiple inputs and are usually unknown. ANNs are commonly shown as networks of interconnected "neurons" that may converse with one another [29]. Neural networks are capable of learning and adapting to inputs because their connections can be changed to correspond to numerical weights. Maximum power points cannot be detected by conventional MPPT methods, which also react slowly to abrupt changes in temperature and light intensity. The three layers that make up an ANN are the hidden, input, and output layers. As inputs are received, the input layer distributes them to the hidden layer's synapses [30]. The output layer generates the precise ANN outcome. The intermediary computations from input to output are carried out via a hidden layer. Five neurons make up the hidden layer of this work, two neurons in the input layer, and two neurons in the output layer. Using this method, maximum voltage and current are acquired as the output, while temperature and irradiance are collected as inputs. The ANN model's structure is shown in Figure 2.

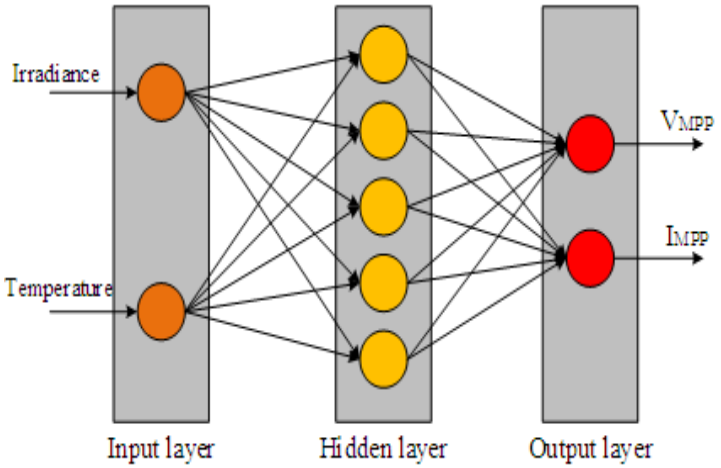

Figure 2: Structure of ANN model

The input parameter used for ANN is formulated using the below equation;

$$IR = IR_{MIN} + \left[R \times \left(IR_{MAX} - IR_{MIN}\right)\right] \qquad (3)$$

$$T = \left[R \times \left(T_{MAX} - T_{MIN}\right)\right] + T_{MIN} \qquad (4)$$

The maximum output voltage obtained using this method is mathematically represented as follows;

Journal of Information Systems Engineering and Management
2024, 9(4)
e-ISSN: 2468-4376
https://www.jisem-journal.com/

Research Article

$$V_{MPP} = V_{MP} + \alpha \times (T - T_S) \qquad (5)$$

Where, IR indicates irradiance, IR_{MAX} denotes maximum irradiance, IR_{MIN} represent minimum irradiance range, R states the random value, T indicates temperature, T_{MAX} means maximum temperature, T_{MIN} specifies minimum temperature, V_{MP} shows maximum voltage age at MPP, α indicates voltage temperature coefficient, and T_S denotes standard temperature [31]. The search for the operating point at which the PV panel may capture its maximum power is the goal of this ANN-based technique [32]. The neural network optimizes each power point by focusing on the DC-DC converter duty ratio and providing a duty ratio for every change in solar temperature and irradiance. The artificial neural network and duty ratio are trained for various temperatures and solar irradiance levels using Levenberg-Marquardt training techniques. Thus, the ANN-based MPPT approach yields the desired results.

3.3 Modelling of 31 level asymmetrical MLI

Figure 3 depicts the suggested 31-level inverter with 8 switches and 3 voltage sources. The DC voltage sources in this topology, also referred to as asymmetrical voltage sources, are unrelated to one another. These asymmetric DC voltage sources are connected to metal oxide semiconductor field effect transistor (MOSFET) unidirectional switches. If a high enough voltage is given to the gate, it can only conduct current in one direction from the source to the drain.The three DC voltage sources in this system need to differ based on the source ratio in order to provide the precise 31-level values. The elements of the suggested inverter structure were the asymmetric voltage sources in the ratio of 1:2:3 for V1:V2:V3. Additionally, the voltage sources are chosen so that the output step voltage reaches the desired level. The voltage sources' chosen values are 100V, 200V, and 300V for V1, V2, and V3, respectively.

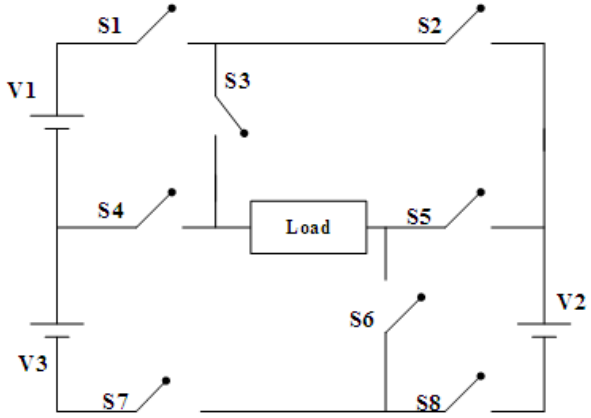

Figure 3: Proposed 31 level inverter

Table 2 shows the recommended MLI's output voltage levels and switching states. The switches' on and off states are denoted by the digits 1 and 0, respectively. Figure 4 shows the numerousoperationalmanners of the suggested 31-level MLI.

Table 2: Switching pulses for proposed MLI

S1	S2	S3	S4	S5	S6	S7	S8	Vout
1	0	1	0	1	0	1	1	15Vdc
0	1	1	0	1	0	1	0	14Vdc
1	0	0	1	1	0	1	0	13Vdc
0	1	0	1	0	1	1	0	12Vdc
1	0	1	0	0	1	0	1	11Vdc
1	1	0	1	0	1	0	1	10Vdc

Journal of Information Systems Engineering and Management
2024, 9(4)
e-ISSN: 2468-4376
https://www.jisem-journal.com/

Research Article

1	0	0	1	1	0	0	1	9Vdc
0	1	0	1	1	0	0	1	8Vdc
1	0	1	0	1	0	1	0	7Vdc
0	1	1	0	0	1	1	0	6Vdc
1	1	0	1	1	0	0	0	5Vdc
0	1	0	1	0	1	1	0	4Vdc
1	0	1	0	1	0	0	1	3Vdc
0	1	1	0	1	0	0	1	2Vdc
1	0	0	1	1	0	0	1	1Vdc
0	1	1	0	1	0	0	0	0Vdc
1	0	0	1	0	1	0	1	-1Vdc
0	1	1	0	0	1	1	0	-2Vdc
1	0	1	0	0	1	1	0	-3Vdc
0	1	0	1	1	0	1	0	-4Vdc
1	0	0	1	1	0	1	0	-5Vdc
0	1	1	0	1	0	0	1	-6Vdc
1	0	1	0	0	1	0	1	-7Vdc
0	1	0	1	0	1	0	1	-8Vdc
1	0	0	1	0	1	0	1	-9Vdc
0	1	1	0	1	0	1	0	-10Vdc
1	0	1	0	1	0	1	0	-11Vdc
0	1	0	1	1	0	1	0	-12Vdc
1	0	0	1	0	1	1	0	-13Vdc
0	1	1	0	0	1	0	1	-14Vdc
1	0	1	0	0	1	0	1	-15Vdc

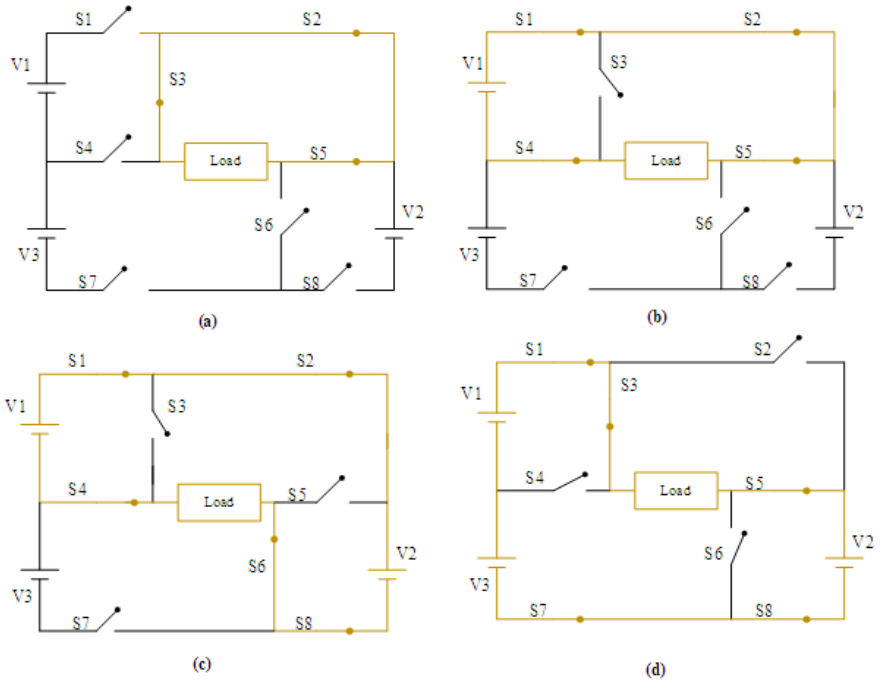

Figure 4: Modes of operations (a) Mode-1 (b) Mode-2 (c) Mode-3 (d) Mode-4

The proposed MLI's operational modes are shown in Figure 4. Figure 4(a) depicts the modes of operation for the zero voltage range; in this mode, S2, S3, and S5 are in the ON position and the remaining switches are in

Journal of Information Systems Engineering and Management
2024, 9(4)
e-ISSN: 2468-4376
https://www.jisem-journal.com/

Research Article

the OFF position. S1, S2, S4, and S5 switches in mode-2 are in the ON state, while the remaining switches are in the OFF state. In mode 2, the output voltage is generated from a single voltage source, yielding an output value of 100V. In mode -3, V1 and V2 are conducted to produce an output voltage of 300V, while S1, S2, S4, S6, and S8 are in the OFF state. In mode 4, the output voltage of 400V at level 31 is obtained by conducting all three voltage sources.

3.4 Proposed C-FOPID-PI controller

The cascaded controller is a two-loop system with benefits over single-loop systems. In this case, the inner loop reduces the effects of the internal process while the outer loop controls the system's final output. Figure 5 depicts the proposed cascaded controller topology. The FOPID [33] controller's outer loop is used in this investigation, and its inner loop is connected to the PI [34] controller. The proposed cascaded controller is used to control the power flow from battery and photovoltaic cells to meet demand. Also, this controller optimally controls the switching pulses of the proposed MLI to reduce THD.

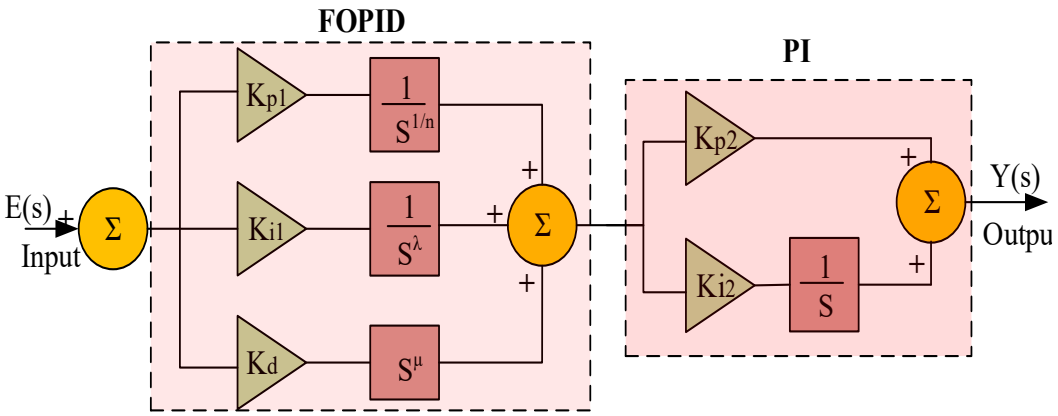

Figure 5: Proposed C-FOPID-PI controller

Equation below states the PID controller's transfer function

$$y(s) = K_{p1} + \frac{K_{i1}}{S} + K_d\, S \qquad (6)$$

The FOPID controller's transfer function can be expressed as follows;

$$y_1(s) = K_{p1} + \frac{K_{i1}}{S^{\lambda}} + K_d\, S^{\mu} \qquad (7)$$

The PI controller transfer function is written as below;

$$y_2(s) = K_{p2} + \frac{K_{i2}}{S} \qquad (8)$$

The suggested controller's transfer function is as follows;

$$Y_{FOPID-PI}(s) = \left(K_{p1} + \frac{K_{i1}}{S^{\lambda}} + K_d\, S^{\mu} \right) * \left(K_{p2} + \frac{K_{i2}}{S} \right) \qquad (9)$$

Where, K_{p1} denotes proportional coefficient, K_{i1} indicates integral gain coefficient of FOPID controller, K_d represent derivative gain coefficient, K_{p2} signifies proportional gain constant for PI, K_{i2} indicates integral gain value for PI controller, λ and μ are fractional order operators which is in the range of [0, 1]. The gain parameters used for this work are as follows: $K_{p1} = 0.2$, $K_{i1} = 0.5$, $K_d = 0.03$, $K_{p2} = 0.2$, $K_{i2} = 0.5$. The phase margin for this work is $\phi_m = 60^o$, and the exponent values are $\lambda = \mu = 0.5$ [35]. To satisfy the

Research Article

load demand, this controller optimally regulates both the PV battery's power flow and the proposed MLI. Additionally, this controller lowers the harmonics in the proposed inverter. The integral error signal determines a controller's output. To regulate the proposed MLI, these pulses are fed into apulse width modulation (PWM) system. PWMcontrols the switching pulse for the inverter switches in an ideal way, minimizing harmonics.

3.5. Power loss analysis

Losses tend to occur in the many components that make up the power circuit while it is operating. These losses fall into two categories: switching loss (P_S), and conduction loss (P_C). Of these losses, the semiconductor is responsible for the conduction and switching losses, while the capacitors are in charge of the ripple losses. Consequently, the circuit's total loss (PTotal) is provided as

$$P_T = P_C + P_S \qquad (11)$$

3.6.1. Conduction Loss

Using (12) the P_C for m power switches in the circuit can be calculated.

$$P_C = \sum_{j=1}^{m} I_{ON}^2 R_{ON} \qquad (12)$$

In the above equation, the on state current flow through the respective power switch is represented by I_{ON} and the internal switch resistance is denoted by R_{ON} .

3.6.2. Switching loss

The ideal switch has 0% switching loss, however because switches aren't perfect, switching loss always occurs. This occurs as a result of current and voltage overlapping when the switch is transitioning. The following mathematical relation provides it.

$$P_S = \left\{ \sum_{j=1}^{m} \sum_{within1/F_0} \frac{V_{ON} I_{ON} T_{ON}}{6} + \frac{V_{OFF} I_{OFF} T_{OFF}}{6} \right\} \times F_0 \qquad (13)$$

Here $V_{ON} I_{ON} T_{ON}$ stand for the voltage, current and duration of the switch's on state, respectively, whereas $V_{OFF} I_{OFF} T_{OFF}$ stand for the switch's off state. Here F_0 indicates the output frequency.

4. Results and Discussion

The model is shown in Figure 6, and the MATLAB/SIMULINK platform is used to verify the suggested work. The organized MLI's output as well as solar power generation in terms of current, voltage, and power generation, will be measured. The proposed inverter and controller were verified on a single-phase microgrid system powered by solar and battery electricity. Table 3 provides the Simulink model's design parameters.

Journal of Information Systems Engineering and Management
2024, 9(4)
e-ISSN: 2468-4376
https://www.jisem-journal.com/

Research Article

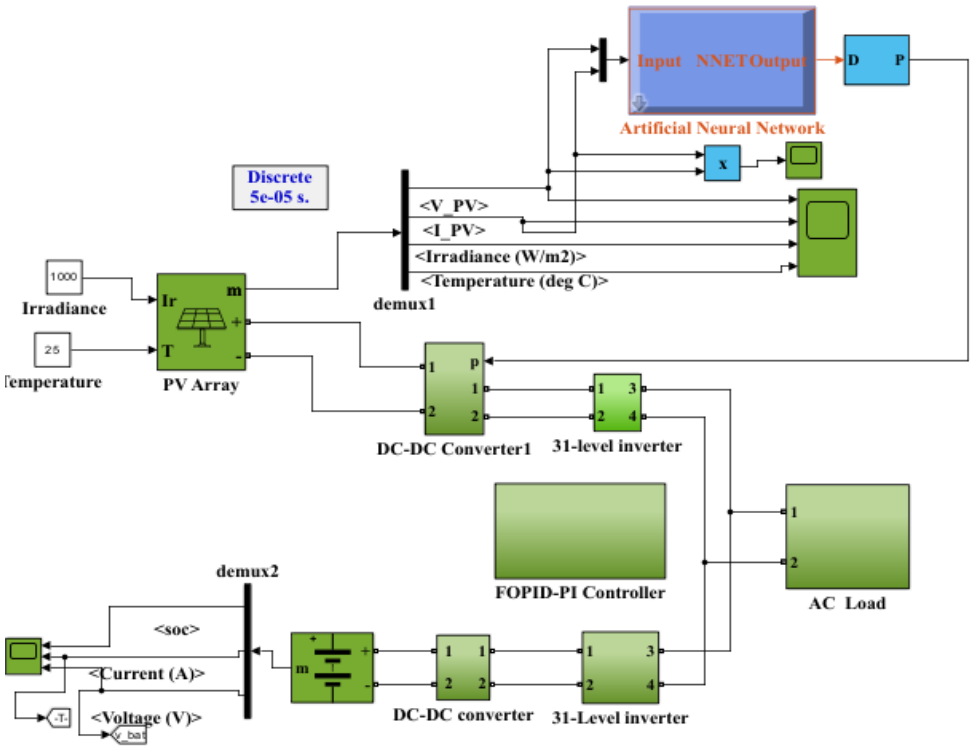

Figure 6: Simulink model of proposed work

Table 3: Simulink Parameters

Parameters	**Values**
Open circuit voltage	38V
Short circuit current	7.89A
Nominal power of the solar PV	320W
Voltage at peak point	32V
Current at peak point	7.55A
DC link voltage	220V
Battery nominal voltage	200V
Rated capacity	14Ah
Filter inductance	1.8mH
Filter capacitance for battery	4µH
Filter capacitance for PV	27µH

Under these conditions, the solar PV is exposed to a constant temperature of 25°C and 250 W/m². Two parallel strings, each with two modules connected in parallel, constitute the solar system. Figure 7 displays the characteristic response derived for factors like current and voltage. PV has a variable voltage that starts at zero and stays at 30 V. Similarly, a photovoltaic system's current changes from 0 to 3.5 A, where it stays constant. As a result, the solar system produces the energy needed to load demand and charge a battery.Therefore the proposed approach effectively ensures system stability.

Journal of Information Systems Engineering and Management
2024, 9(4)
e-ISSN: 2468-4376
https://www.jisem-journal.com/

Research Article

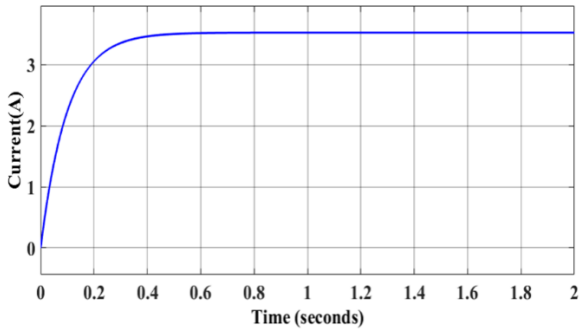

(a)

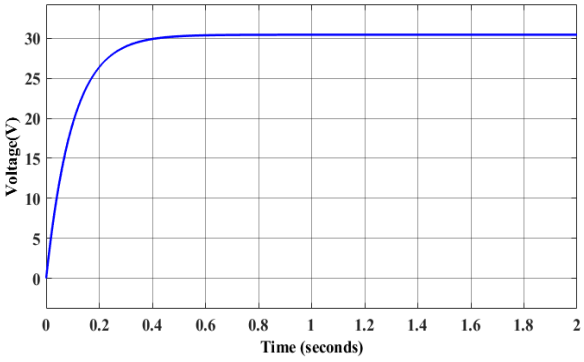

(b)

Figure 7: Solar PV model (a) current and (b) voltage

The DC link is connected to solar power to produce the necessary electricity. The solar panel's voltage and current are sent into an ANN-based MPPT controller to set the duty cycle at the best possible value. Figure 8 displays the total power from PV and DC link voltage under a continuous solar source.These results demonstrates the panel effectively enhance the voltage and current which improves the stability.

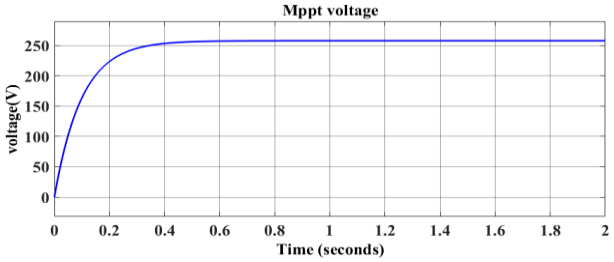

(a)

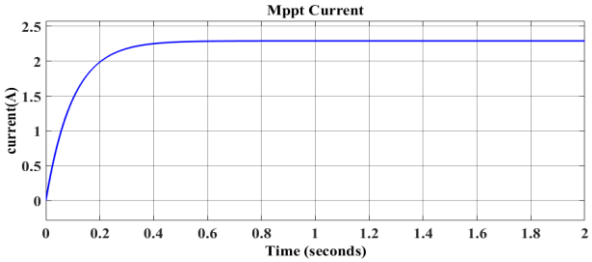

(b)

Figure 8: MPPT output (a) voltage and (b) current

Journal of Information Systems Engineering and Management
2024, 9(4)
e-ISSN: 2468-4376
https://www.jisem-journal.com/

Research Article

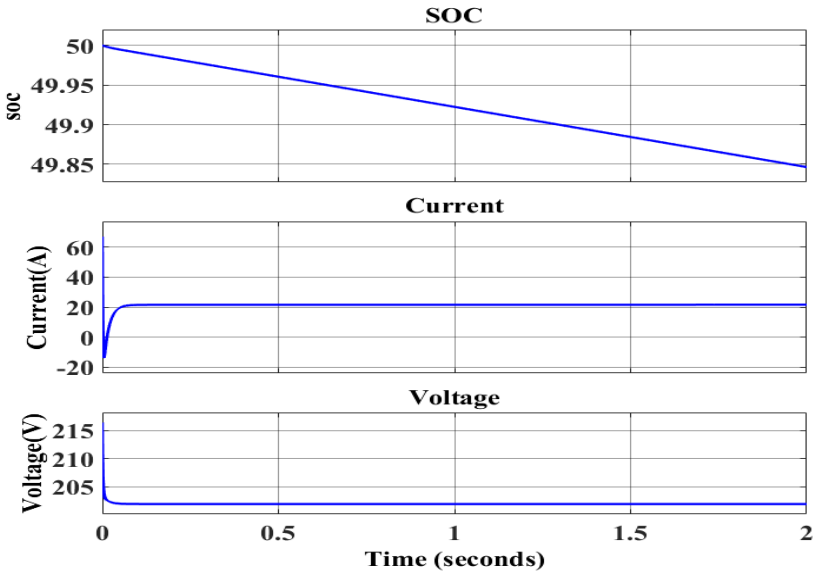

Figure 9: Output of battery source

PV sources store their excess power in batteries for later utilization. If the source produces insufficient power to satisfy load demands, the battery is depleted. The discharged battery is depicted in Figure 9 with respect to voltage, current, and state of charge. The inverter receives the optimized power via an ANN-based MPPT for power conversion. The 31 level inverter is suggested here to enhance harmonics, and stability.

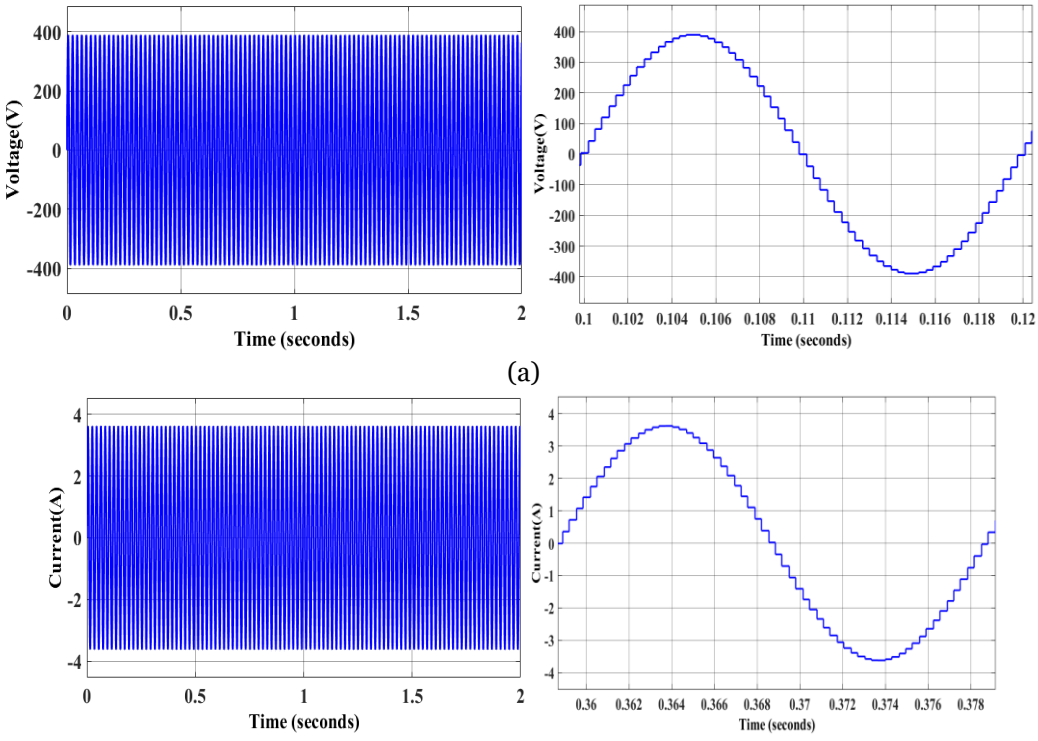

Figure 10: Output of proposed 31-level inverter for R load (a) Voltage (b) Current

Figure 10 displays the output from the proposed inverter with a resistive (R) load. The inverter's voltage and current are 400V and 3.8A, respectively, as can be seen. Figure 11 displays the output voltage and current for the suggested MLI in an inductive load. In this instance, the current is 4.2A, and the inverter voltage is 400V.

Journal of Information Systems Engineering and Management
2024, 9(4)
e-ISSN: 2468-4376
https://www.jisem-journal.com/

Research Article

In this work, the inductive (L) load value is 20mH.These MLI demonstrates superior stability under varying load and supply conditions.

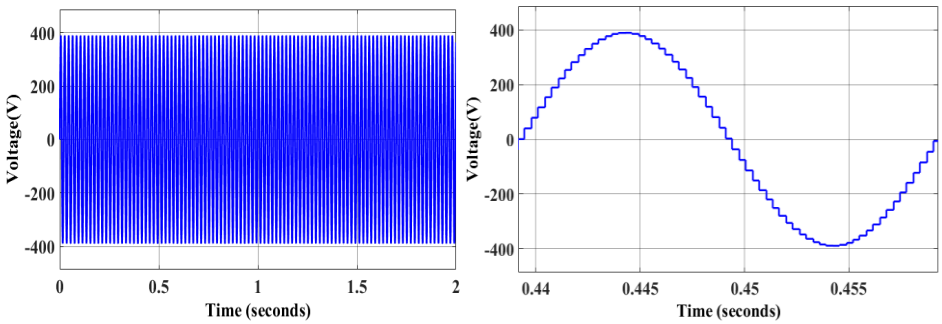

(a)

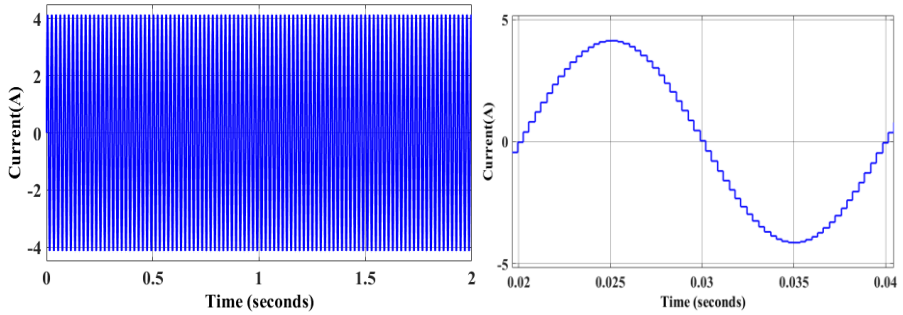

(b)

Figure 11: (a) Voltage **(b)** current waveform for proposed MLI in L load

The efficiency of the suggested 31-level inverter with the cascaded FOPID-PI controller is shown in Figure 12. Here, the THD for both the voltage and current signals is quantified using the fundamental frequency of 50 Hz. THD for voltage is 2.95%, whereas THD for the suggested inverter is 0.76% for current.

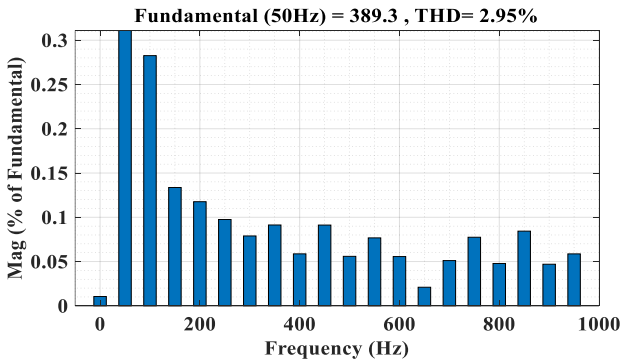

(a)

Journal of Information Systems Engineering and Management
2024, 9(4)
e-ISSN: 2468-4376
https://www.jisem-journal.com/

Research Article

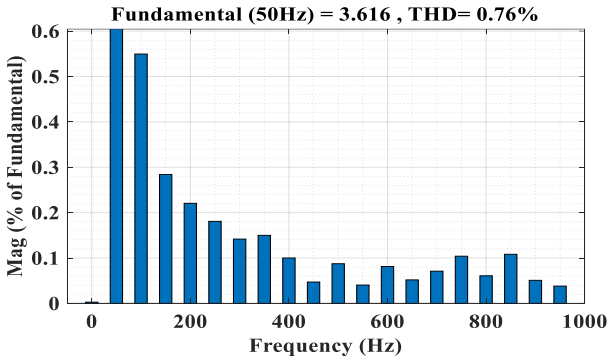

(b)

Figure 12: FFT analysis of proposed inverter for (a) voltage, (b) current

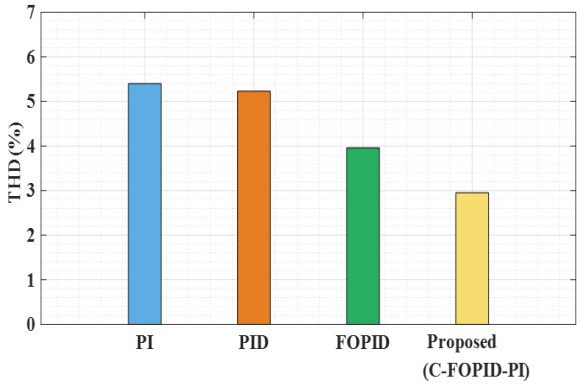

Figure 13: Comparison of the proposed controller

The power system in an islanded microgrid system improves the stability since the proposed controller exhibits the least amount of distortion. Consequently, the suggested MLI is more suited for the suggested cascaded tuned controller. Figure 13 displays the corresponding THD results for the controller and the controllers that are currently in use. For this comparison, the suggested controller is contrasted with the PI, PID, and FOPID controllers. THD was obtained by the FOPID controller at 3.96%, the PID controller at 5.23%, and the PI controller at 5.40%. The comparison of proposed controller is shown in Figure 13. Compared to other controllers, the proposed controller produced lower THD. Current controllers are inserted into the proposed model and produce the appropriate outcomes. The efficiency of the suggested MLI will rise with the addition of this proposed controller; The proposed technique maintain the stability compared to other conventional techniques.

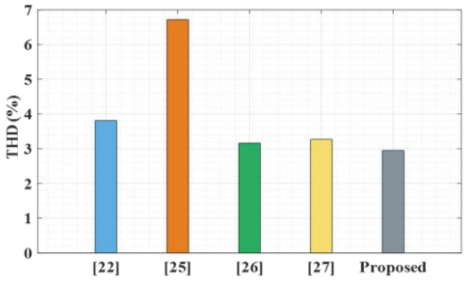

(a)

Journal of Information Systems Engineering and Management
2024, 9(4)
e-ISSN: 2468-4376
https://www.jisem-journal.com/

Research Article

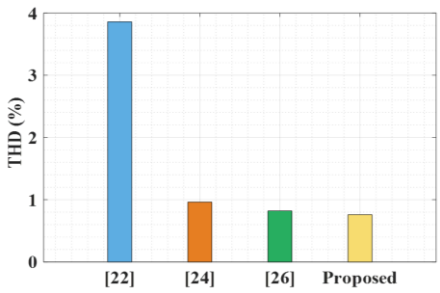

(b)

Figure 14: Comparison of THD with existing works (a) voltage (b) current

Figure 14 shows how THD compares to previous research. In this comparison, 31 level inverter voltage THD values from [22], [25], [26], and [27] are used. The 31 level inverter produced a THD of 2.98% less using this proposed way, which is less than the current MLI topology. Figure 14 (b) compares the current THD values of 31-level inverters [22], [24], and [26].
Consequently, the performance of the proposed C-FOPID-PI controller and 31-level MLI is assessed using a range of outcomes, and the THD response is compared with that of established methods. The outcome validates the effectiveness of the suggested 31-level MLI and controller.

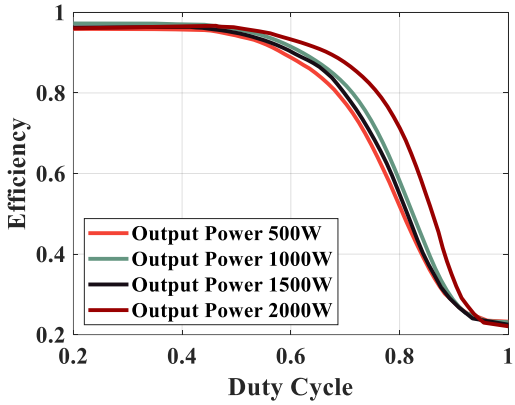

Figure 15: Analysis efficiency with duty cycle

Figure 15 shows the analysis of efficiency with duty cycle. The duty cycle and efficiency ranges from 0.2 to 1. Here the duty cycle is calculated at different power values like 500W, 1000W, 1500W, 2000W. For 2000W the efficiency is very higher when compared to other power. This demonstrates the model performance better.

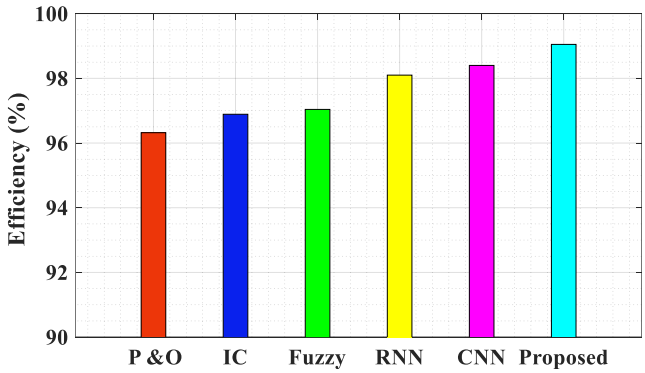

Figure 16: Comparison of efficiency with proposed and existing methods

Journal of Information Systems Engineering and Management
2024, 9(4)
e-ISSN: 2468-4376
https://www.jisem-journal.com/

Research Article

Figure 16 shows the comparison of efficiency with proposed and existing methods. The proposed method achieves the efficiency of 99.05%, P & O achieves the efficiency of 96.32%, ICachieves the efficiency of 96.89%,Fuzzy achieves the efficiency of 97.04%,RNN achieves the efficiency of 98.1%, and CNN achieves the efficiency of 98.14%. Here the proposed approach achieves the better efficiency which shows the stable performance.

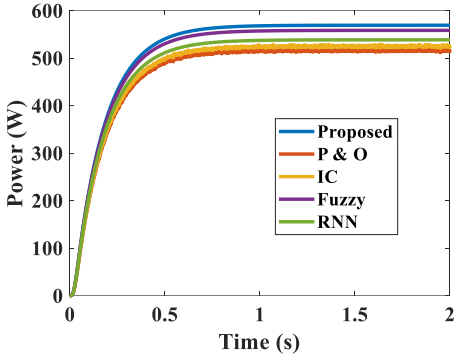

Figure 17: Comparison of MPPT power with proposed and existing methods

Figure 17 shows the comparison of MPPT power with proposed and existing methods. The MPPT power is compared with four existing techniques like P &O, IC, Fuzzy and RNN. The power ranges from 0 to 600W and the time ranges from 0 to 2 sec. The proposed method track more power when compared to other conventional techniques. The proposed method tracks nearly 550W of power which very high which demonstrates high efficiency performance. Table 4 shows the loss and total power of R and L load for the proposed work.

Table 4: Loss and Total power of R and L load for the proposed work

Parameters	**R-Load**	**L-Load**
V_{rms}	363.9V	363V
I_{rms}	3.6A	4.14A
Conduction Loss	14.80W	22.20W
Switching Loss	4.34W	4.34W
Total Loss	19.14W	26.54W
Output power	1310.04W	1502.82W
Efficiency	98.66%	98.38%

The proposed model achieves the conduction loss of 14.80W for R load and 22.20W for L load.The proposed model achieves the switching loss of 4.34W for R load and 4.34W for L load. It achieves the efficiency of 98.66% for R-load and 98.38% for L load. These results demonstrates the high efficiency, indicates minimal energy dissipation, effective power conversion and stable operation.

5. Conclusion

A unique 31-level MLI with a control method for single phase microgrid systems is proposed in this publication. This paper proposes an MPPT-based ANN to track the PV panel's maximum power. The suggested 31-level asymmetrical inverter is used to convert DC to AC. In this study, a unique topology for producing 31 levels in the inverter output is proposed. It is suggested that the inverter get optimal switching pulses from the cascaded FOPID-PI controller. The results of applying the suggested technique to a single-phase microgrid system with the MATLAB/Simulink tool are shown. There are as few DC sources and switches as possible in the design of the 31 level inverter. The suggested approach yields an efficiency of 99.05% and a THD of 2.95% for the voltage signal and 0.75% for the current signal. For R and L loads, respectively, the suggested model yields a total loss of 19.14W and 26.54W. These findings demonstrate the

effectiveness of the suggested method for enhancing the stability of a single-phase microgrid system with better dependability and power quality. The use of a variety of controllers in subsequent projects ensures that PQ will improve.

Funding Information: No funding is provided for the preparation of manuscript.

Reference

[1] Shahnia F, Chandrasena RP. A three-phase community microgrid comprised of single-phase energy resources with an uneven scattering amongst phases. *International Journal of Electrical Power & Energy Systems*. 2017;84:267-83.
[2] Thirunavukkarasu GS, Seyedmahmoudian M, Jamei E, Horan B, Mekhilef S, Stojcevski A. Role of optimization techniques in microgrid energy management systems—A review. *Energy Strategy Reviews*. 2022;43:100899.
[3] Avramidis II, Evangelopoulos VA, Georgilakis PS, Hatziargyriou ND. Demand side flexibility schemes for facilitating the high penetration of residential distributed energy resources. *IET Generation, Transmission & Distribution*. 2018;12(18):4079-88.
[4] Datta U, Kalam A, Shi J. A review of key functionalities of battery energy storage system in renewable energy integrated power systems. Energy Storage. 2021;3(5):e224.
[5] Micallef A. Review of the current challenges and methods to mitigate power quality issues in single-phase microgrids. *IET Generation, Transmission & Distribution*. 2019;13(11):2044-54.
[6] Alhaiz HA, Alsafran AS, Almarhoon AH. Single-Phase Microgrid Power Quality Enhancement Strategies: A Comprehensive Review. *Energies*. 2023;16(14):5576.
[7] Elfaleh I, Abbassi F, Habibi M, Ahmad F, Guedri M, Nasri M, Garnier C. A comprehensive review of natural fibers and their composites: an eco-friendly alternative to conventional materials. *Results in Engineering*. 2023:101271.
[8] Kurian GM, Jeyanthy PA, Devaraj D. FPGA implementation of FLC-MPPT for harmonics reduction in sustainable photovoltaic system. *Sustainable Energy Technologies and Assessments*. 2022;52:102192.
[9] Chitransh A, Kumar S. The different type of MPPT techniques for photovoltaic system. *Indian Journal of Environment Engineering (IJEE)*. 2021;1(2):1-4.
[10] Kumari A, Gopal Y, Dhaked DK, Panda KP, Kumar YV. A single source five-level switched-capacitor based multilevel inverter with reduced device count. *e-Prime-Advances in Electrical Engineering, Electronics and Energy*. 2023;5:100235.
[11] Mahesh PV, Meyyappan S, Alla RK. A new multivariate linear regression MPPT algorithm for solar PV system with boost converter. *ECTI Transactions on Electrical Engineering, Electronics, and Communications*. 2022;20(2):269-81.
[12] Ahmad W, Qureshi MB, Khan MM, Fayyaz MA, Nawaz R. Optimizing Large-Scale PV Systems with Machine Learning: A Neuro-Fuzzy MPPT Control for PSCs with Uncertainties. *Electronics*. 2023;12(7):1720.
[13] Mahalakshmi G, Kumar SA, Abhisek K, Arthi J, Ellanchikkumar T. Hybrid Power Management Using Interleaved Landsman Converter Implemented Through Machine Learning. In *2023 4th International Conference on Signal Processing and Communication (ICSPC)*. 2023:38-42. IEEE.
[14] Srivastava S, Lata C, Lohan P, Mosobi RW. Comparative Analysis of Particle Swarm Optimization and Artificial Neural Network Based MPPT with Variable Irradiance and Load. *IJEER*. 2022;10(3):460-5.
[15] Khemili FZ, Bouhali O, Lefouili M, Chaib L, El-Fergany AA, Agwa AM. Design of Cascaded Multilevel Inverter and Enhanced MPPT Method for Large-Scale Photovoltaic System Integration. *Sustainability*. 2023;15(12):9633.
[16] Rana RA, Patel SA, Muthusamy A, Lee CW, Kim HJ. Review of multilevel voltage source inverter topologies and analysis of harmonics distortions in FC-MLI. *Electronics*. 2019;8(11):1329.
[17] Kaliannan T, Albert JR, Begam DM, Madhumathi P. Power quality improvement in modular multilevel inverter using for different multicarrier PWM. *European journal of electrical engineering and computer Science*. 2021;5(2):19-27.

Research Article

[18] Kumar PV, Venkateshwarlu S. Analysis of Switching Losses in Multilevel Cascaded H-bridge and Diode-Clamped Inverter. *CVR Journal of Science and Technology*. 2020;19(1):1-6.
[19] Prasad D, Dhanamjayulu C. Solar PV-fed multilevel inverter with series compensator for power quality improvement in grid-connected systems. *IEEE Access*. 2022;10:81203-19.
[20] Bajaj M, Singh AK. Grid integrated renewable DG systems: A review of power quality challenges and state-of-the-art mitigation techniques. *International Journal of Energy Research*. 2020;44(1):26-69.
[21] Nahin NI, Biswas SP, Mondal S, Islam MR, Muyeen SM. A Modified PWM Strategy With an Improved ANN Based MPPT Algorithm for Solar PV Fed NPC Inverter Driven Induction Motor Drives. *IEEE Access*. 2023.
[22] Kumar N, Siddiqui AS, Singh R. ANFIS BASED MPPT AND CASCADED H-BRIDGE, 31-LEVEL MLI WITH HIGH GAIN LANDSMAN CONVERTER IN SINGLE-PHASE SPV POWER WITH GRID CONNECTIVITY FOR IMPROVING POWER QUALITY. *Journal of Data Acquisition and Processing*. 2023;38(2):3838.
[23] Prathaban AV, Karthikeyan D. Grey wolf optimization-recurrent neural network based maximum power point tracking for photovoltaic application. *Indonesian Journal of Electrical Engineering and Computer Science (IJEECS)*. 2022;26(2):629-38.
[24] Kurian GV, Jeyanthy PA, Devaraj D. Efficient evaluation of anticipated 31-level inverter for photovoltaic energy system with reduced switches. *Sustainable Computing: Informatics and Systems*. 2022;36:100797.
[25] Akther S, Talukder P, Dey MC, Begum A, Rashid MM. Designing a Novel 31-Level Asymmetrical Multilevel Inverter Topology with Comparative Analysis. In *2022 International Conference on Advancement in Electrical and Electronic Engineering (ICAEEE)*. 2022:1-6. IEEE.
[26] Shah MJ, Pandya KS, Chauhan P. An MPPT-based 31-Level ADC Controlled Micro-Inverter. *Engineering, Technology & Applied Science Research*. 2022;12(5):9149-54.
[27] Krishnamoorthy U, Pitchaikani U, Rusu E, Fayek HH. Performance Analysis of Harmonic-Reduced Modified PUC Multi-Level Inverter Based on an MPC Algorithm. *Inventions*. 2023;8(4):90.
[28] Gulzar MM, Iqbal A, Sibtain D, Khalid M. An innovative converterless solar PV control strategy for a grid connected hybrid PV/wind/fuel-cell system coupled with battery energy storage. *IEEE Access*. 2023;11:23245-59.
[29] Balakishan P, Chidambaram IA, Manikandan M. An ANN Based MPPT for Power Monitoring in Smart Grid using Interleaved Boost Converter. *Tehnički vjesnik*. 2023;30(2):381-9.
[30] Ibrahim NF, Mahmoud MM, Al Thaiban AM, Barnawi AB, Elbarbary ZS, Omar AI, Abdelfattah H. Operation of grid-connected PV system with ANN-based MPPT and an optimized LCL filter using GRG algorithm for enhanced power quality. *IEEE Access*. 2023.
[31] Bouakkaz MS, Boukadoum A, Boudebbouz O, Bouraiou A, Attoui I. ANN based MPPT algorithm design using real operating climatic condition. In *2020 2nd international conference on mathematics and information technology (ICMIT)*. 2020:159-163. IEEE.
[32] Hussain MT, Sarwar A, Tariq M, Urooj S, BaQais A, Hossain MA. An Evaluation of ANN Algorithm Performance for MPPT Energy Harvesting in Solar PV Systems. *Sustainability*. 2023;15(14):11144.
[33] Tufenkci S, Alagoz BB, Senol B, Matušů R. An overview of FOPID controller design in v-domain: design methodologies and robust controller performance. *International Journal of Systems Science*. 2023;54(11):2316-36.
[34] Mallempati SK, Satheesh G, Peddakotla S. Design of optimal PI controller for torque ripple minimization of SVPWM-DTC of BLDC motor. *International Journal of Power Electronics and Drive Systems*. 2023;14(1):283.
[35] Kumar VA, Mouttou A. Improved performance with fractional order control for asymmetrical cascaded H-bridge multilevel inverter. *Bulletin of Electrical Engineering and informatics*. 2020;9(4):1335-44.
[37] Praveena, A., and K. Sathishkumar. "Power quality improvement using a 31-level multi-level inverter with bio-inspired optimization approach." Frontiers in Energy Research 12 (2024): 1264157.